The Cdc42 GEF Intersectin 2 controls mitotic spindle orientation to form the lumen during epithelial morphogenesis

Alejo E. Rodriguez-Fraticelli,[1] Silvia Vergarajauregui,[1] Dennis J. Eastburn,[2] Anirban Datta,[2] Miguel A. Alonso,[1] Keith Mostov,[2] and Fernando Martín-Belmonte[1]

[1]Centro de Biología Molecular Severo Ochoa, Consejo Superior de Investigaciones Científicas, Madrid 28049, Spain
[2]Department of Anatomy, University of California, San Francisco, San Francisco, CA 94143

Epithelial organs are made of tubes and cavities lined by a monolayer of polarized cells that enclose the central lumen. Lumen formation is a crucial step in the formation of epithelial organs. The Rho guanosine triphosphatase (GTPase) Cdc42, which is a master regulator of cell polarity, regulates the formation of the central lumen in epithelial morphogenesis. However, how Cdc42 is regulated during this process is still poorly understood. Guanine nucleotide exchange factors (GEFs) control the activation of small GTPases. Using the three-dimensional Madin–Darby canine kidney model, we have identified a Cdc42-specific GEF, Intersectin 2 (ITSN2), which localizes to the centrosomes and regulates Cdc42 activation during epithelial morphogenesis. Silencing of either Cdc42 or ITSN2 disrupts the correct orientation of the mitotic spindle and normal lumen formation, suggesting a direct relationship between these processes. Furthermore, we demonstrated this direct relationship using LGN, a component of the machinery for mitotic spindle positioning, whose disruption also results in lumen formation defects.

Introduction

During development, epithelial cells develop apicobasal polarity, a specific type of constitutive cell polarity which is regulated by different mechanisms, including membrane transport, cytoskeleton organization, and cellular junction formation (Bryant and Mostov, 2008). The deregulation of apicobasal polarity is associated with major diseases such as polycystic kidney disease and cancer (Lee and Vasioukhin, 2008). Rho GTPases are molecular switches that control a wide variety of signaling pathways critical for the acquisition of the polarized phenotype. For instance, the orientation of epithelial cell polarity is controlled by the opposing actions of Rac1 and RhoA (O'Brien et al., 2001; Yu et al., 2003, 2005, 2008). Cdc42, which is a master regulator of cell polarity, controls the formation of a single lumen in MDCK cells. For this, Cdc42 is activated at the apical plasma membrane in a pathway regulated by annexin2 (Anx2) and PTEN, which mediate the enrichment of phosphatidylinositol-4,5-bisphosphate (PtdInsP2) at the apical domain (Martín-Belmonte et al., 2007). Additionally, Cdc42 activity has also been shown to regulate epithelial morphogenesis by controlling other processes such as vesicle traffic and exocytosis (Kroschewski et al., 1999; Müsch et al., 2001; Rojas et al., 2001; Wu et al., 2008) and, more recently, the mitotic spindle orientation (Jaffe et al., 2008). Therefore, Cdc42 appears to control different pathways and/or mechanisms for epithelial morphogenesis. How Cdc42 is regulated during these processes is currently unknown.

Rho guanine nucleotide exchange factors (GEFs) constitute the main activators of Rho GTPases. Rho GEFs are multidomain proteins modulated by different signals, whose number in the human genome greatly exceeds the number of Rho family proteins. This suggests that different Rho GEFs could be regulating where and how a Rho GTPase is activated to control different cellular processes (Jaffe and Hall, 2005). Intersectin (ITSN) is a multimodular protein that is mainly expressed in two splicing variants: ITSN short (ITSN-S) and ITSN long (ITSN-L). Only

Correspondence to Fernando Martín-Belmonte: fmartin@cbm.uam.es

Abbreviations used in this paper: DIC, dynein intermediate chain; Dox, doxycycline; EH, Eps15 homology; GEF, guanine nucleotide exchange factor; ITSN, Intersectin; KD, knockdown; MT, metaphase time; MTOC, microtubule-organizing center; N-WASP, neural WASP; vhITSN2, Venus–human ITSN2; WASP, Wiskott-Aldrich syndrome protein.

The Rockefeller University Press $30.00
J. Cell Biol. Vol. 189 No. 4 725–738
www.jcb.org/cgi/doi/10.1083/jcb.201002047

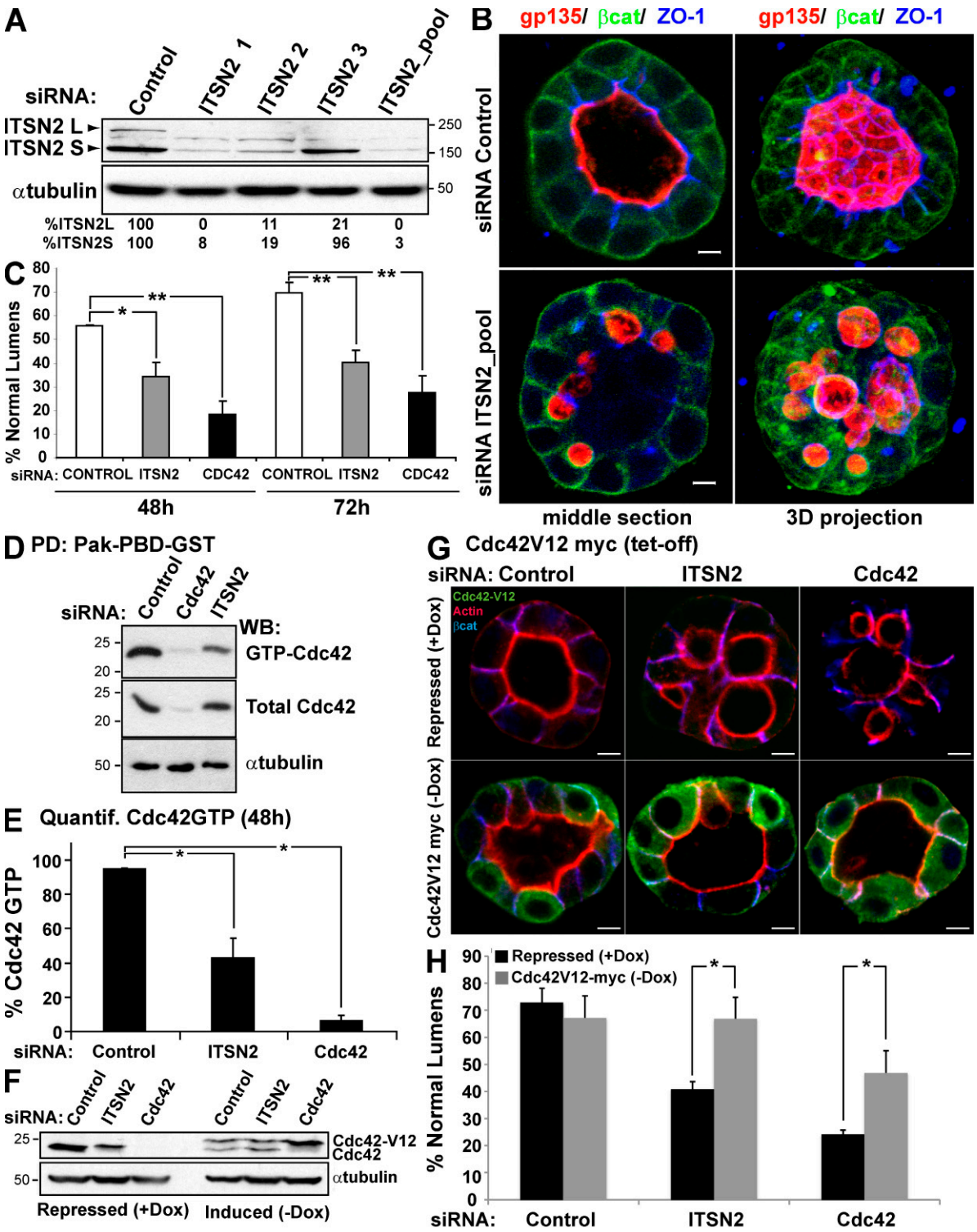

Figure 1. **ITSN2 silencing abrogates lumen formation and reduces GTP-bound Cdc42 levels.** (A) Down-regulation of ITSN2 by siRNA. MDCK cells were transfected with siRNA ITSN2-1, ITSN2-2, ITSN2-3, and a pooled combination of all three or with control siRNA and allowed to form cysts for 72 h. Total lysates were blotted for ITSN2 and tubulin. (B) Confocal microscopy images of the effect of ITSN2 siRNA–mediated silencing on lumen formation. Cells were transfected with ITSN2 siRNA pool or control siRNA and plated to form cysts for 72 h. Cells were stained to detect gp135, β-catenin (βcat), and ZO-1. (C) Quantification of cysts with normal lumens in cells transfected with control siRNA, Cdc42 siRNA, or ITSN2 siRNA pool. Values are mean ± SD from five different experiments (n = 100 cysts/experiment; *, $P < 0.05$; **, $P < 0.005$). (D) siRNA-mediated silencing of ITSN2 inhibits activation of Cdc42. Cells were transfected with ITSN2 siRNA pool, Cdc42 siRNA, or control siRNA. Extracts from these cells were pulled down with Pak-PBD-GST. Total and GTP-bound Cdc42 was detected by immunoblotting with specific antibodies to Cdc42 or tubulin. PD, pull-down; WB, Western blot. (E) Quantification of Cdc42-GTP levels in ITSN2-silenced cells. The ratios of GTP-bound to total protein were calculated relative to tubulin content. Values shown are mean ± SD from three different experiments (*, $P < 0.005$). (F) Down-regulation of ITSN2 by siRNA in cells with the inducible expression of Cdc42V12-myc. MDCK cells stable expressing Cdc42V12-myc under the control of the tet-off repressor were transfected with siRNA to ITSN2 pool or Cdc42 or with control siRNA and allowed to form cysts for 72 h in the presence of Dox (Cdc42V12-myc expression repressed) or not (induced). Total lysates were Western blotted for

ITSN-L contains the Dbl domain at the C-terminal region of ITSN and functions as a specific GEF for Cdc42 (Hussain et al., 2001). ITSN-L has two isoforms in mammals, ITSN1-L, which is differentially expressed in brain, and ITSN2-L, which is ubiquitously expressed (Pucharcos et al., 2000). ITSN interacts with Wiskott-Aldrich syndrome protein (WASP) and neural WASP (N-WASP) through its SH3 domains to trigger actin polymerization together with Cdc42 (Hussain et al., 2001; McGavin et al., 2001; Irie and Yamaguchi, 2002). ITSNs have been proposed to be a connection between endocytosis and exocytosis because they bind to multiple endocytic and exocytic proteins such as dynamin and SNAP25 and -23 (Okamoto et al., 1999). In fact, the ability of ITSNs to interact with multiple components suggests that they might act as scaffolding proteins necessary for the formation of signaling platforms.

In this work, we have characterized ITSN2 as a specific GEF for Cdc42 activation in epithelial morphogenesis using the organotypic 3D MDCK cell system. We have found out that ITSN2 localizes to centrosomes and is required for the correct orientation of the mitotic spindle and for correctly positioning the apical surface during epithelial morphogenesis. In addition, we have demonstrated a direct relation between lumen formation and spindle orientation. Disruption of LGN, a component of the machinery which regulates spindle movements and orientation, interferes with lumen formation in MDCK cells forming cysts.

Results

ITSN2 is required for normal lumen morphogenesis

In our previous work, we have described that Cdc42 must be activated to induce the formation of the apical domain and the central lumen in 3D MDCK cysts (Martín-Belmonte et al., 2007). A candidate screening for Cdc42 GEFs using RNAi was performed to identify Cdc42-specific GEFs associated with epithelial lumen formation using the apical marker gp135/podocalyxin and the actin cytoskeleton integrity as readout to detect luminal defects in the 3D MDCK model. Using this system, ITSN2 emerged as a candidate for regulating the Cdc42 activity controlling lumen formation (unpublished data). To confirm the function of ITSN2, we designed three siRNA heteroduplexes to deplete endogenous ITSN2 levels. The siRNA directed against the C-terminal region (ITSN2-3) specifically reduced the levels of the long isoform, whereas siRNAs ITSN2-1 and ITSN2-2, directed against the middle and N-terminal region of ITSN2, respectively, were able to reduce the expression of both isoforms (Fig. 1 A). The pool of the three siRNAs dramatically reduced both isoforms as well (Fig. 1 A) and was used for all of the following experiments to silence ITSN2. When siRNA-transfected cells were plated to form cysts, most control cells formed normal lumens at 72 h (70%; Fig. 1 B); MDCK cysts with reduced ITSN2 formed cysts of similar size, but only 41% of them had normal lumens at 72 h. Instead, most cysts with reduced ITSN2 had multiple small lumens, although the basolateral marker β-catenin and tight junctions marker ZO-1 localized normally (Fig. 1, B and C). This phenotype very closely resembles that obtained by silencing Cdc42 in MDCK cysts (Fig. 1 C; Martín-Belmonte et al., 2007). To further confirm these results, we prepared RNAi pPRIME lentiviral system carrying short hairpin RNAs targeted specifically to silence the canine isoform of ITSN2 and obtained consistent results (Fig. S1). To investigate the GEF function of ITSN2 in 3D MDCK cysts, we analyzed GTP-bound Cdc42 levels in ITSN2 and Cdc42 knockdown (KD) cells by GST pull-down assays. Cells silenced for ITSN2 showed a significant reduction in Cdc42-GTP levels, which might explain the aberrant phenotype observed in cyst morphogenesis (Fig. 1, D and E; and Fig. S1 D).

To confirm the specificity of ITSN2 function on Cdc42 activation, we prepared MDCK cells expressing the constitutively active form of Cdc42, Cdc42V12-GFP under the control of a tetracycline-repressible promoter (tet-off; Fig. 1 F), and we tested the ability for lumen formation in ITSN2- and Cdc42-silenced cells. The expression of Cdc42V12 was able to restore the normal formation of the lumen in cells silenced for ITSN2 and also, although to lesser extent, of cells silenced for Cdc42 (Fig. 1, G and H). Together, these results suggest that ITSN2 is required for the activation of Cdc42 to form the lumen.

ITSN2 localizes at centrosomes

Next, we characterized the localization of ITSN2 in MDCK cysts. Staining with several antibodies available for ITSN2 did not serve to identify the localization of the endogenous protein (unpublished data). Therefore, we prepared MDCK cells stably expressing a fusion of the fluorescent protein Venus and human ITSN2 (vhITSN2). In interphase cells, vhITSN2 localized to intracellular clusters close to the apical membrane, which was stained with the apical marker gp135 in MDCK cysts (Fig. 2 A, arrows). vhITSN2 colocalized with the centrosomal markers pericentrin (Fig. 2 B, arrows) and γ-tubulin (not depicted). In mitotic cells, vhITSN2 also distributed at the edge of the spindle poles, stained with acetylated tubulin (Fig. 2 C, arrows), and colocalized with the centrosomal marker pericentrin (not depicted). Because vhITSN2 is an siRNA-resistant form of ITSN2 (Fig. 2 D), we used these cells to validate the specific effect of ITSN2 silencing on lumen formation. We observed that vhITSN2 expression restored the normal phenotype in lumen formation in cells silenced for endogenous ITSN2 (Fig. 2, E and F).

To confirm that the localization of ITSN2 to centrosomes was not an artifact caused by the ectopic expression of vhITSN2, we obtained centrosome-enriched fractions of MDCK cells using centrifugation in Ficoll gradients (Blomberg-Wirschell

Cdc42 and α-tubulin. (A, D, and F) Molecular mass is indicated in kilodaltons. (G) Confocal microscopy images of the rescue effect of Cdc42V12-myc in cells silenced for ITSN2, Cdc42, or control on lumen formation. Cells were transfected with ITSN2 pool, control, or Cdc42 siRNAs and plated to form cysts for 72 h in the presence (Cdc42V12 repressed) or the absence (induced) of 20 µmol Dox. Cells were stained to detect actin, Cdc42V12-myc, and β-catenin. (H) Quantification of cysts with normal lumens in cells expressing or not Cdc42V12-myc and transfected with the control, Cdc42, or ITSN2 pool siRNAs. Values are mean ± SD from three different experiments ($n \geq 100$ cysts/experiment; *, $P < 0.005$). Bars, 5 µm.

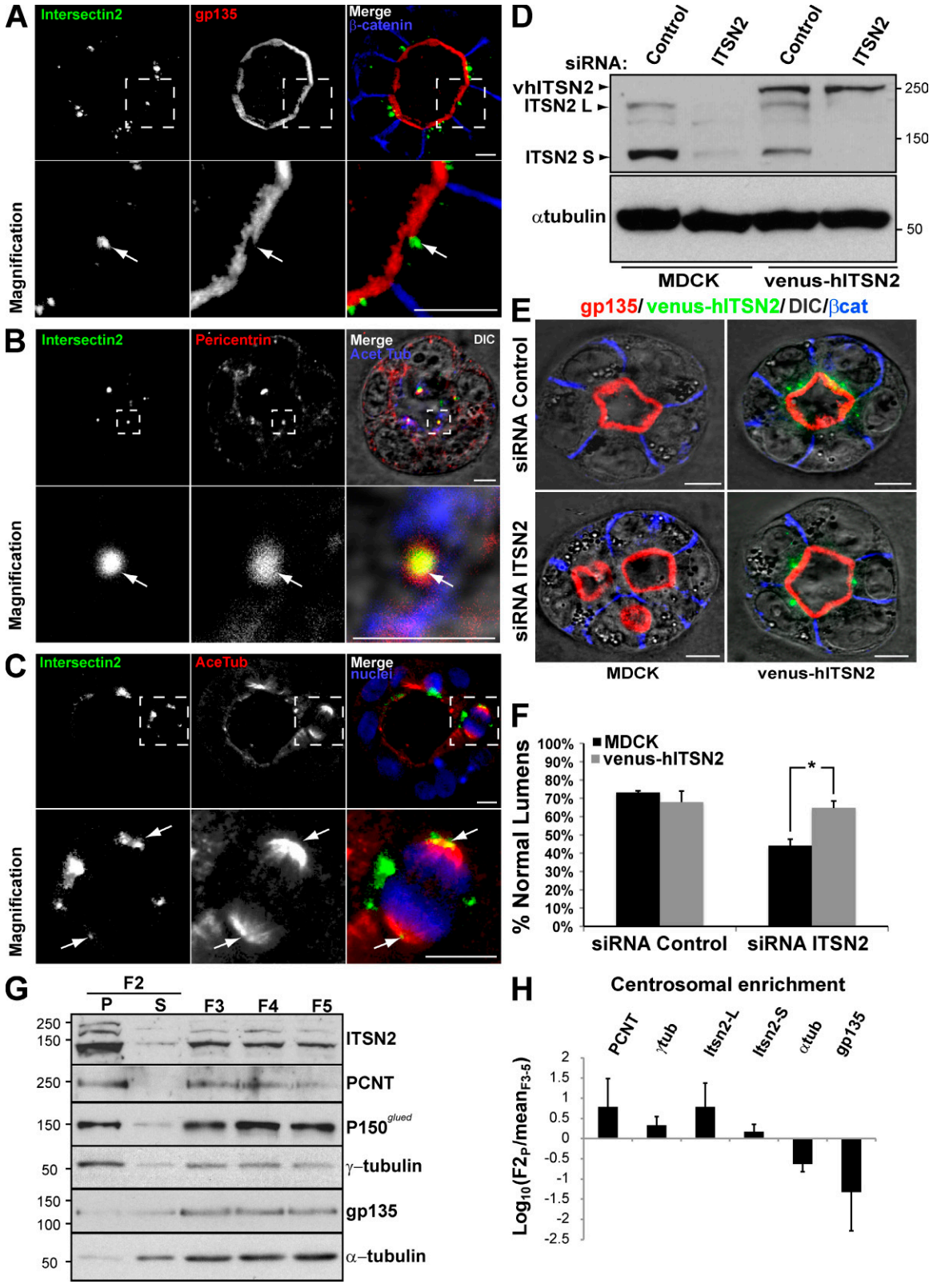

Figure 2. **The siRNA-resistant form of ITSN2, vhITSN2, rescues normal lumen formation.** (A) vhITSN2 is apically localized in MDCK cysts. Cells expressing vhITSN2 (green) were plated to form cysts for 72 h. Cysts were stained with gp135 and β-catenin (top). (B) ITSN2 colocalizes with pericentrin at centrosomes in interphase MDCK cells. Cells expressing vhITSN2 (green; left) were stained with pericentrin (centrosomal marker; middle) and acetylated tubulin (Acet Tub; right with DIC and merge). (C) ITSN2 localizes at spindle poles in mitotic MDCK cells. Cells expressing vhITSN2 (green; left) were stained with acetylated tubulin (AceTub; middle) and chromatin (blue; right and merge). (A–C) Bottom panels show the magnification image of the boxed areas indicated in the top panels. Arrows indicate ITSN2 localization. (D) Down-regulation of ITSN2 by siRNA in cells stably expressing vhITSN2. MDCK cells stable expressing vhITSN2 were transfected with siRNA to ITSN2 pool or with control siRNA and allowed to form cysts for 72 h. Total lysates were blotted for ITSN2 and α-tubulin. (E) Confocal microscopy images of the rescue effect of vhITSN2 in cells silenced for ITSN2 on lumen formation. Cells stably expressing

and Doxsey, 1998). We detected endogenous ITSN2 in the sediments positive for γ-tubulin/pericentrin and negative for α-tubulin/gp135 (Fig. 2 G, left lane, F2-P). The quantitative analysis showed that both ITSN isoforms (ITSN2-L and ITSN2-S) were highly enriched in the centrosomal fraction together with other centrosomal proteins (Fig. 2 H). To characterize whether the association of centrosomes with ITSN2 is dependent on its association with microtubules or, conversely, whether ITSN2 associates with centrosomes independently of the microtubules, we performed depolymerization/repolymerization experiments using nocodazole (Hung et al., 2000). Microtubules were depolymerized using nocodazole for 4 h, and the subsequent pattern of microtubule regrowth was determined (Fig. S2 A). In nocodazole, interphase microtubules were depolymerized. However, compared with untreated cells, no significant decrease in the concentration of ITSN2 was observed in nocodazole-treated cells (Fig. S2 A). To ensure that ITSN2 is indeed located at the centrosomes where microtubule growth is initiated, the nocodazole-treated cells were washed out to permit microtubule regrowth. After increasing times of regrowth (0–45 min), cells were fixed and stained to detect α- and γ-tubulin, and confocal images were analyzed. As shown in Fig. S2 A, microtubule growth started at the centrosomes, where ITSN2 is located.

Altogether, these results indicate that ITSN2 localizes to centrosomes, and it could activate Cdc42 in this region to form the lumen. Because Cdc42 regulates cell polarity through different effectors that control vesicle trafficking, actin organization, and microtubule stabilization (Etienne-Manneville, 2004), we next focused on characterizing the process in which ITSN2 activates Cdc42.

The exocytosis of apical gp135/podocalyxin and apical junction formation are both dependent on Cdc42 but independent of ITSN2

Activated Cdc42 can associate with numerous effectors that regulate vesicle traffic, mainly through the regulation of the actin cytoskeleton. Accumulated evidence supports the idea that ITSNs are adaptors that coordinate Cdc42-dependent membrane trafficking events in different cells (Hussain et al., 2001; Irie and Yamaguchi, 2002; Malacombe et al., 2006). To evaluate whether ITSN2 functions in exocytosis during lumen formation, we analyzed apical vesicle exocytosis using calcium switch experiments. For these experiments, we used MDCK stably expressing GFP-tagged Anx2 (Anx2-GFP), a peripheral membrane protein which associates with the plasma membrane in a calcium-dependent manner (Rescher and Gerke, 2004), and the apical marker gp135/podocalyxin. Control or MDCK cells silenced for ITSN2 or Cdc42 were polarized in monolayers. After 48 h, the cells were treated overnight with normal (Fig. 3 A) or low-calcium medium (Fig. 3 B). Low-calcium conditions induced the internalization of the apical protein gp135 and Anx2-GFP in a vesicular apical compartment (Fig. 3 B), as described previously (Vega-Salas et al., 1987, 1988). The restitution of normal calcium levels induced the exocytic translocation of gp135 and Anx2-GFP to the plasma membrane in control cells (Fig. 3 C). In contrast, Cdc42 KD cells did not restore the apical compartment after returning to normal calcium conditions (Fig. 3 C), inducing a phenotype very similar to that produced by silencing Cdc42 in the 3D MDCK cyst model (Martín-Belmonte et al., 2007, 2008). Importantly, the restitution of normal calcium levels in ITSN2 KD cells resulted in normal exocytosis of gp135 and Anx2-GFP to the plasma membrane (Fig. 3 C). Previous experiments have shown that activated Cdc42 is implicated in the formation of normal tight junctions at epithelial cell–cell contacts (Joberty et al., 2000; Hurd et al., 2003; Wells et al., 2006). To test whether ITSN2 could activate Cdc42 to form apical junctions, we performed a calcium switch experiment and analyzed the recovery of transepithelial resistance in vivo using an electrical cell-substrate impedance system (Lo et al., 1995). Again, the recovery of normal transepithelial resistance levels was delayed in cells knocked down for Cdc42, whereas cells knocked down for ITSN2 showed a recovery profile similar to that of control cells (Fig. 3 D). Furthermore, the staining of the tight junction protein ZO-1 also showed a specific effect of Cdc42 in the recovery of tight junction integrity in the calcium switch experiment (Fig. 3, A–C). Finally, we also observed that ITSN2 and Cdc42 were not implicated in the orientation of the microtubule-organizing center (MTOC; Fig. S3, A and B) or in the formation of the primary cilium (not depicted). These results suggest that ITSN2 activation of Cdc42 does not affect either vesicle trafficking or tight junction formation in MDCK cell morphogenesis.

With the goal of identifying the possible role of Cdc42 in which ITSN2 is involved during the process of lumen formation, we further investigated the phenotypes of ITSN2 KD and Cdc42 KD in MDCK cysts. First, we quantified the proportion of internal vesicles with apical markers and intercellular lumens in siRNA-transfected cells. For this quantification, we assumed that the intracellular lumens were similar to the vesicular apical compartments that appeared in the calcium switch experiments (Fig. 3 B) and, therefore, could indicate flaws in the process of exocytosis. ITSN2 KD cysts had a significantly reduced proportion of intracellular gp135-loaded vesicles compared with Cdc42 KD cysts, which contained both intercellular lumens and intracellular gp135-loaded vesicles (Fig. 3, E and F). Collectively,

vhITSN2 were transfected with ITSN2 pool or control siRNAs and plated to form cysts for 72 h. Cells were stained to detect gp135, vhITSN2, and β-catenin (βcat). (F) Quantification of cysts with normal lumens in cells expressing vhITSN2 and transfected with the control or ITSN2 pool siRNAs. Values are mean ± SD from three different experiments ($n \geq 100$ cysts/experiment; *, $P < 0.005$). (G) Endogenous ITSN2 is present in centrosome-enriched fractions. MDCK cells were plated to reach confluence and then treated with 0.3 µM nocodazole and 1 µg/ml cytochalasin D for 4 h. A rapid isolation of centrosomes was performed using Ficoll gradient centrifugation of lysates, and then, centrosomes in the F2 fraction were precipitated by ultracentrifugation. The F2 supernatant (S) and pellet (P) were loaded together with fractions F3, F4, and F5, containing cytosolic and membrane proteins. The fractions were immunoblotted for ITSN2 and centrosomal, cytosolic, and membrane markers. (D and G) Molecular mass is indicated in kilodaltons. (H) Densitometry quantification of fractional enrichment represented as $\log_{10}(F2_P/mean_{F3-5})$. Values are mean ± SD from three different experiments. PCNT, pericentrin. Bars, 5 µm.

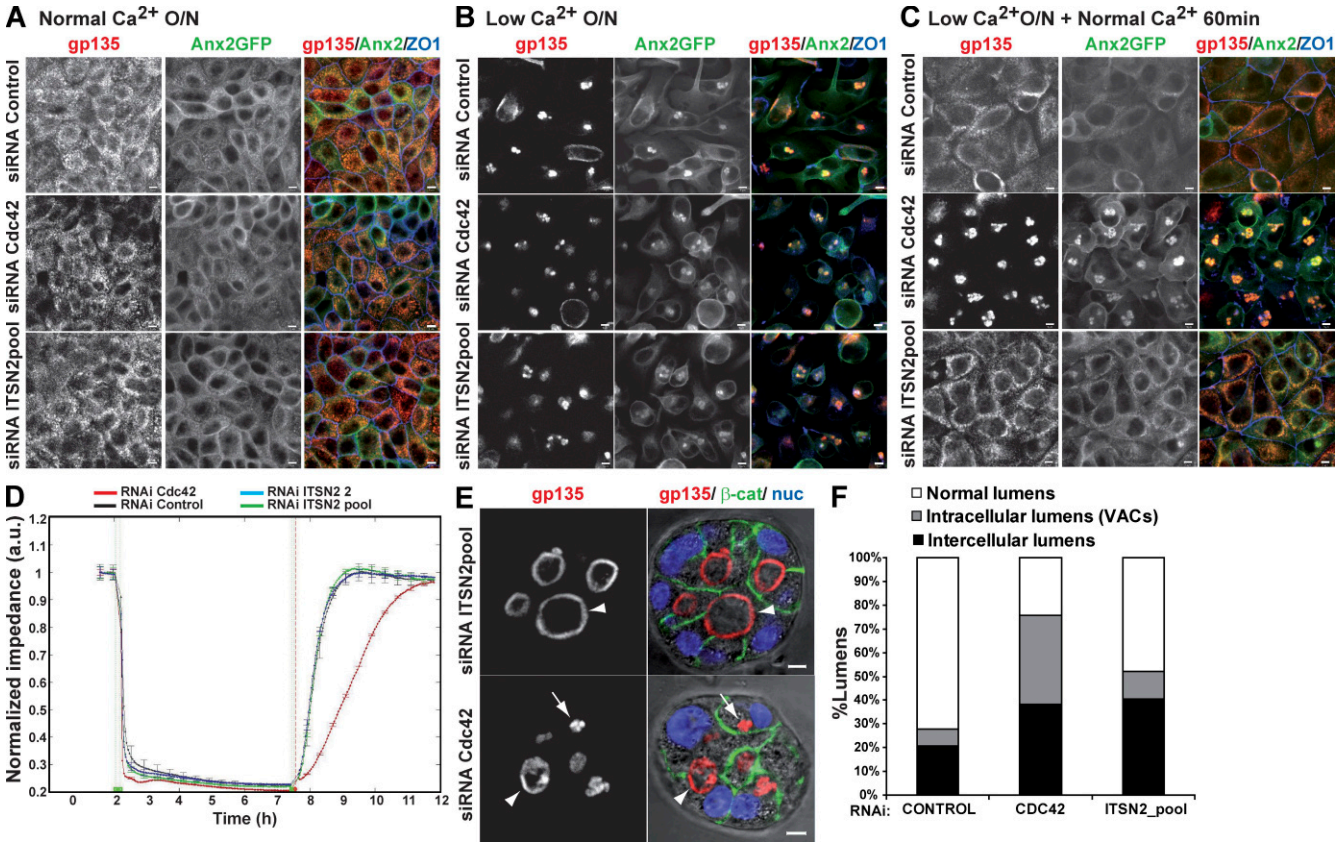

Figure 3. **Apical exocytosis is affected in Cdc42 KD cells but not in ITSN2 KD cells.** (A–C) Effect of Cdc42 and ITSN2 silencing on gp135 and Anx2 exocytosis in calcium switch experiments. Anx2-GFP cells were transfected with Cdc42 siRNA (middle), ITSN2 siRNA pool (bottom) or control siRNA (top) and plated after 48 h to form a confluent monolayer (A). Cells were treated with calcium-free medium overnight (O/N; B) and then treated with complete medium for 60 min (C). Cells were fixed after each step and stained to detect gp135 and ZO-1. (D) Quantification of monolayer impedance. Control (black line)-, Cdc42 (red line)-, and ITSN2-silenced cells (blue and green lines) were plated on electrode plates and allowed to form a confluent monolayer. Cells were treated as described for A–C, and impedance was measured in real time to determine epithelial permeability. Values shown are mean ± SD from three different experiments. (E) Lumen formation phenotypes of Cdc42 and ITSN2 silencing. Cdc42 and ITSN2 KD cells were plated to form cysts for 72 h. Cells were stained to detect gp135 (left), β-catenin (β-cat), and nuclei (nuc). Arrows indicate intracellular lumens (vesicular apical compartments [VACs]), and arrowheads indicate intercellular lumens. (F) Quantification of cysts with normal lumens or with multiple intercellular and intracellular lumens in cells transfected with control siRNA, Cdc42 siRNA, or ITSN2 siRNA pool. Values shown are means from three different experiments ($n \geq 100$ cysts/experiment; *, $P < 0.005$ for intracellular lumens of Cdc42 vs. control or ITSN2; **, $P < 0.06$ for intercellular lumens of ITSN2 vs. control; ***, $P < 0.07$ for intercellular lumens of Cdc42 vs. control). Bars, 5 µm.

these results indicated that ITSN2 does not detectably function to activate Cdc42 for vesicular trafficking or the formation of tight junctions, but it could be necessary for other processes such as mitotic spindle orientation, in which defects in the activation of Cdc42 results in multiple lumen phenotypes.

ITSN2 and CDC42 are both required for normal positioning of the mitotic spindle in 3D MDCK cultures

Recent work performed in Caco-2 epithelial cells suggested that Cdc42 is required for the orientation of the mitotic spindle to position the apical surface in cells forming 3D cysts (Jaffe et al., 2008). We analyzed the orientation of the mitotic spindle in dividing cells using cysts of MDCK cells with reduced levels of Cdc42 or ITSN2 and compared them with control cells. We transfected MDCK cells with control or siRNA heteroduplexes targeting Cdc42 or ITSN2 (Fig. 4 A) and then measured the angle formed between the apicobasal axis and the spindle pole axis in three dimensions, which was calculated as described in the schematic drawing of Fig. 4 B. Most of the mitotic spindles analyzed in control cells were normal (Fig. 4 B, right). However, cysts with reduced levels of both Cdc42 and ITSN2 had a significant increase in abnormally positioned spindle poles, the effect being stronger in cells silenced for Cdc42 (Fig. 4, B [left and middle] and C). These results suggest that the defect in mitotic spindle rotation and/or positioning in cells silenced for Cdc42 might generate the defects observed in lumen formation. To test this hypothesis, we analyzed mitotic spindle dynamics in metaphase by confocal time-lapse microscopy using 3D MDCK cells expressing GFP–α-tubulin. We observed that in control cells, there was an ~90° rotation of the spindle from the apicobasal axis to the plane of the epithelium (Fig. 4 D, top; and Video 1), which was described previously in MDCK cysts (Yu et al., 2003). However, in cells silenced for Cdc42 or ITSN2, there was a disruption of this spindle rotation, which resulted in the translocation of one of the dividing cells to the center of the cyst, narrowing the luminal space (Fig. 4 D, middle and bottom; and Videos 2 and 3). Moreover, the impairment in spindle rotation also induced a delay

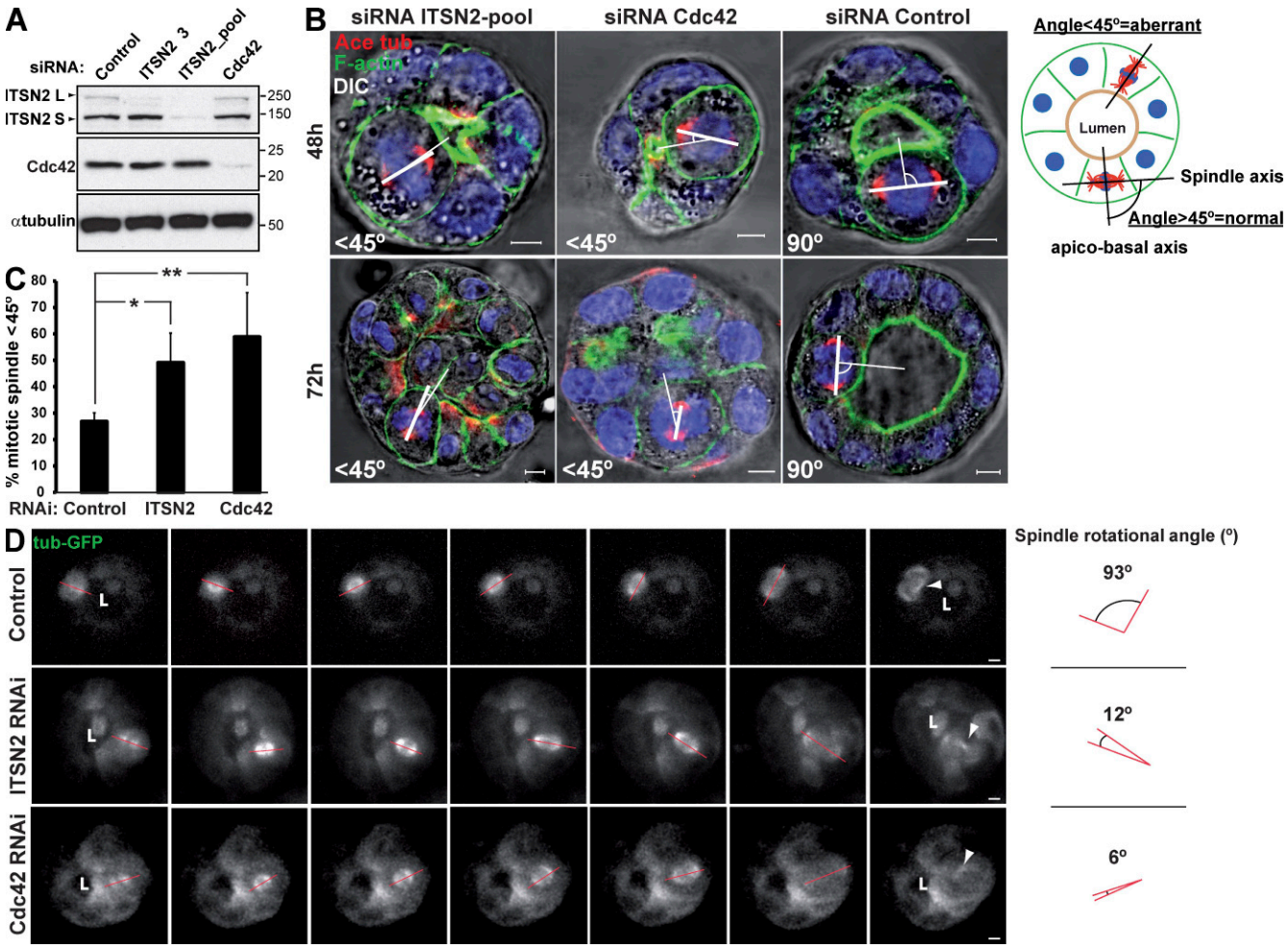

Figure 4. **Cells silenced for Cdc42 or ITSN2 present spindle orientation defects.** (A) Down-regulation of ITSN2 and Cdc42 by siRNA. Cells were transfected with Cdc42, ITSN2, or control siRNA and allowed to form cysts for 72 h, and then total cell lysates were Western blotted for Cdc42 and α-tubulin (control). Molecular mass is indicated in kilodaltons. (B) Effect of Cdc42 and ITSN2 siRNA in spindle orientation. Cells were transfected with ITSN2 siRNA pool (left), Cdc42 siRNA (middle), or control siRNA (right) and plated to form cysts for 48 (top) or 72 h (bottom). Cells were stained to detect actin, acetylated tubulin (Ace tub), and chromatin (blue). The apicobasal axis (thin line) and the spindle axis (thick line) are drawn in white. (C) Quantification of misoriented spindles in 48-h cysts silenced with Cdc42, ITSN2, or control siRNA. The angle between the apicobasal axis and spindle axis was measured. Angles <45° were counted as abnormal. Values shown are mean ± SD from five different experiments (n = 30 cysts/experiment; *, $P < 0.01$; **, $P < 0.05$). (D) Spindle orientation defects in Cdc42- and ITSN2-silenced cells. MDCK cells stably expressing α-tubulin–GFP were transfected with control (top), ITSN2 (middle), or Cdc42 siRNA (bottom) and plated to form cysts. Live cells were analyzed by 3D video confocal microscopy from early metaphase until anaphase at 0.5 frames/min. Quantification of angle deviation in control and cells knocked down for Cdc42 or knocked down for ITSN2 is shown. Arrowheads indicate the localization of the midbodies after cytokinesis. Red lines indicate the orientation of the mitotic spindle. "L" indicates localization of the lumen. Bars, 5 μm.

in the metaphase to anaphase transition, which we characterized in MDCK 2D monolayers for statistics (Fig. S3 C). Metaphase time (MT) was affected in cells silenced for Cdc42 (MT = 27.3 ± 7.7 min) and cells silenced for ITSN2 (MT = 31.2 ± 11.5 min), as compared with control cells (MT = 16.9 ± 4.6 min; Fig. S3, C and D). These results indicate that ITSN2 and Cdc42 are both required for normal mitotic spindle orientation during cell division. In particular, they seem to control the normal rotation of the mitotic spindle in mitotic cells.

In summary, we have shown that ITSN2 activates Cdc42, which in turn controls the orientation of the mitotic spindle during mitosis. Although our results can explain the phenotype of multiple lumens observed in cells silenced for ITSN2 or Cdc42, it sheds no light on the subjacent molecular mechanism. To identify the possible mechanism of action of ITSN2, we characterized the domain responsible for targeting ITSN2 to centrosomes. ITSN2 contains two EH (Eps15 homology) domains, a central coiled-coil region, and five consecutive SH3 domains. Additionally, ITSN-L presents an extended C-terminal region containing a DH (Dbl homology), a PH (pleckstrin homology), and a C2 domain (Fig. 5 A). We prepared GFP-fused constructs comprising different domains of ITSN2 and characterized their subcellular localization in MDCK cells (Fig. 5, A and B). We observed that when overexpressed, the EH domains of ITSN2 targeted GFP to the centrosomes in MDCK cells (Fig. 5 B, left; arrows show the colocalization of EH domains with pericentrin). In contrast, the rest of the domains analyzed distributed in the cytoplasm, forming clumps that did not colocalize with centrosomal markers (Fig. 5 B, bottom right). Previous results have shown the ability of ITSNs to interact with multiple components

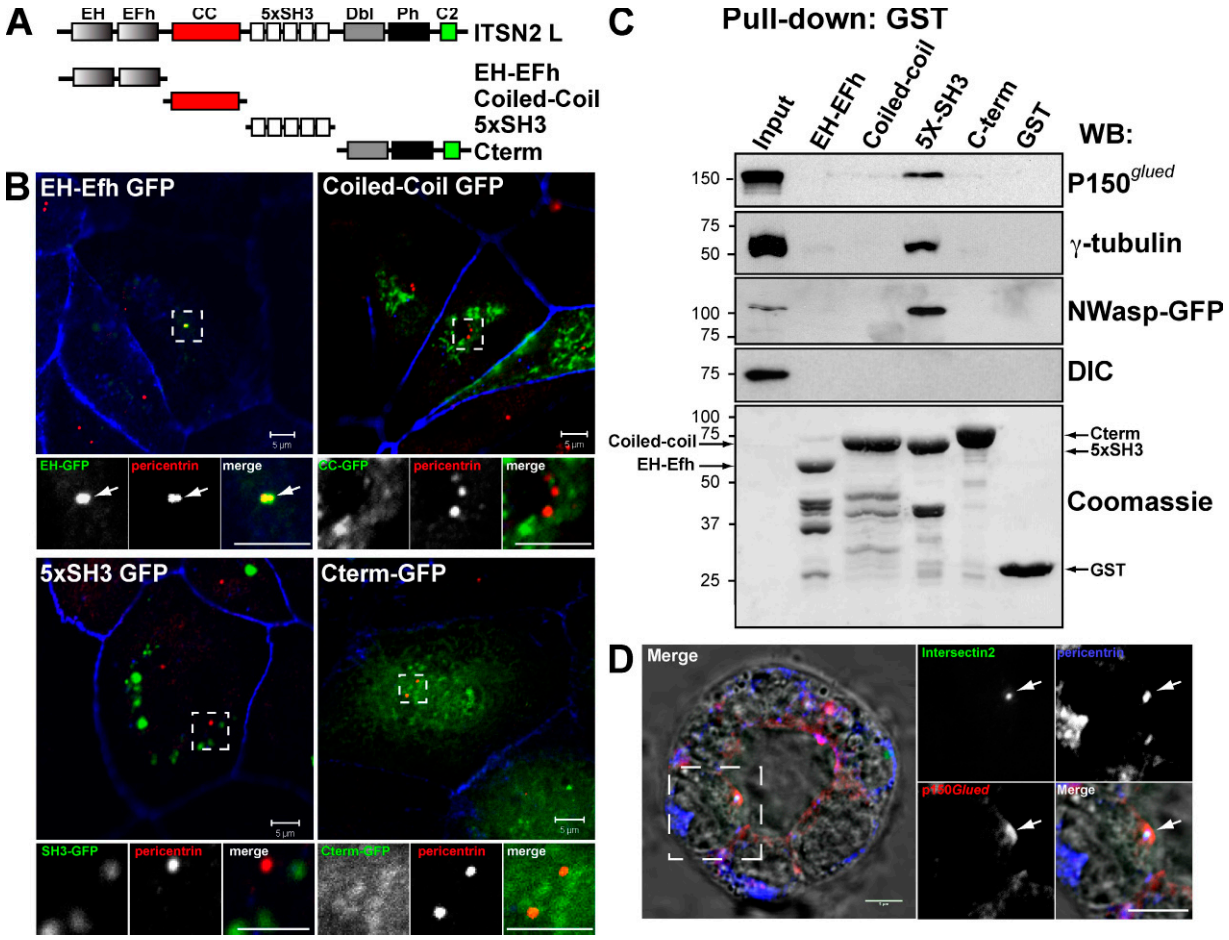

Figure 5. **ITSN2 is partially localized at centrosomes through the EH domains and interacts with centrosomal proteins through the SH3 domains.** (A) Schematic diagram of the different ITSN2-L domains (called EH-EFh, coiled-coil [CC], 5xSH3, and C terminus) and the GFP and GST constructs generated with them. (B) EH-Efh domains target ITSN2 to the centrosomes. MDCK cell were transfected with GFP-tagged protein constructs of ITSN2 (EH, coiled-coil, 5xSH3, and C terminus) and analyzed by confocal microscopy. Cells were stained to detect pericentrin and actin (blue). Bottom panels show the magnification image of the boxed areas indicated in the top panels. Arrows indicate the localization of EH-GFP to the centrosome (pericentrin) (C) ITSN2 interacts with the centrosomal proteins γ-tubulin and $p150^{Glued}$. Total cell lysates were incubated with beads preloaded with GST-tagged protein constructs of ITSN2 (EH, coiled-coil, 5xSH3, and C terminus) or with GST. Pulled down fractions were immunoblotted to detect γ-tubulin, $p150^{Glued}$, N-WASP–GFP (positive control), and DIC or stained with Coomassie blue to detect the total amount of the GST-fused proteins used as bait. Molecular mass is indicated in kilodaltons. WB, Western blot. (D) ITSN2 colocalizes with γ-tubulin and $p150^{Glued}$ in cysts. Cysts expressing vhITSN2 (green) were stained for $p150^{Glued}$ and pericentrin merged with DIC in the left panel. Right panels are the magnification of the boxed area in the left panel. Arrows indicate the colocalization of ITSN2 and $p150^{Glued}$ at the centrosome (pericentrin). Bars, 5 µm.

of the endocytic machinery, which suggests that ITSNs might act as scaffolding proteins necessary for the formation of signaling platforms (Yamabhai et al., 1998; Okamoto et al., 1999; Pucharcos et al., 2000; Hussain et al., 2001). To characterize the possible role of ITSN2 as a scaffolding protein at centrosomes, we performed pull-down assays using GST fusions of the various aforementioned domains of ITSN2 (Fig. 5 A). ITSN2 was found to interact through the SH3 domains with $p150^{Glued}$, one of the subunits of the dynactin complex, and with γ-tubulin but not with other members of the complex such as dynein intermediate chain (DIC; Fig. 5 C). As a control, we analyzed the interaction of ITSN2 with N-WASP through the SH3 domains of ITSN2 (Fig. 5 C), as described previously for ITSN2 and WASP in T cells (McGavin et al., 2001). The dynein–dynactin complex is an essential regulator of spindle orientation and cell division (Quintyne et al., 1999). Previous studies have indicated that Cdc42 activation is involved in the reorientation of the MTOC during cell migration through a pathway dependent on the dynein–dynactin complex (Palazzo et al., 2001; Gomes et al., 2005). We observed that vhITSN2 colocalized with $p150^{Glued}$ and pericentrin at the centrosome in 3D cysts (Fig. 5 D). These results suggest that ITSN2, which is targeted to the centrosome through its EH domains, mediates the activation of Cdc42 in this region, which in turn would control the orientation of the spindle through the activity of other centrosomal proteins such as the dynein–dynactin complex.

Next, we analyzed the localization of Cdc42 in different phases of the cell cycle using MDCK cells expressing Cdc42-GFP (Fig. 6). It has been reported that the localization of Cdc42 is associated with the plasma membrane and the Golgi in different cell types (Itoh et al., 2002; Yoshizaki et al., 2003). The stable expression of Cdc42-GFP caused a significant reduction of the endogenous Cdc42, so the final levels of total Cdc42 were similar to the endogenous protein in these cells (Fig. 6 B).

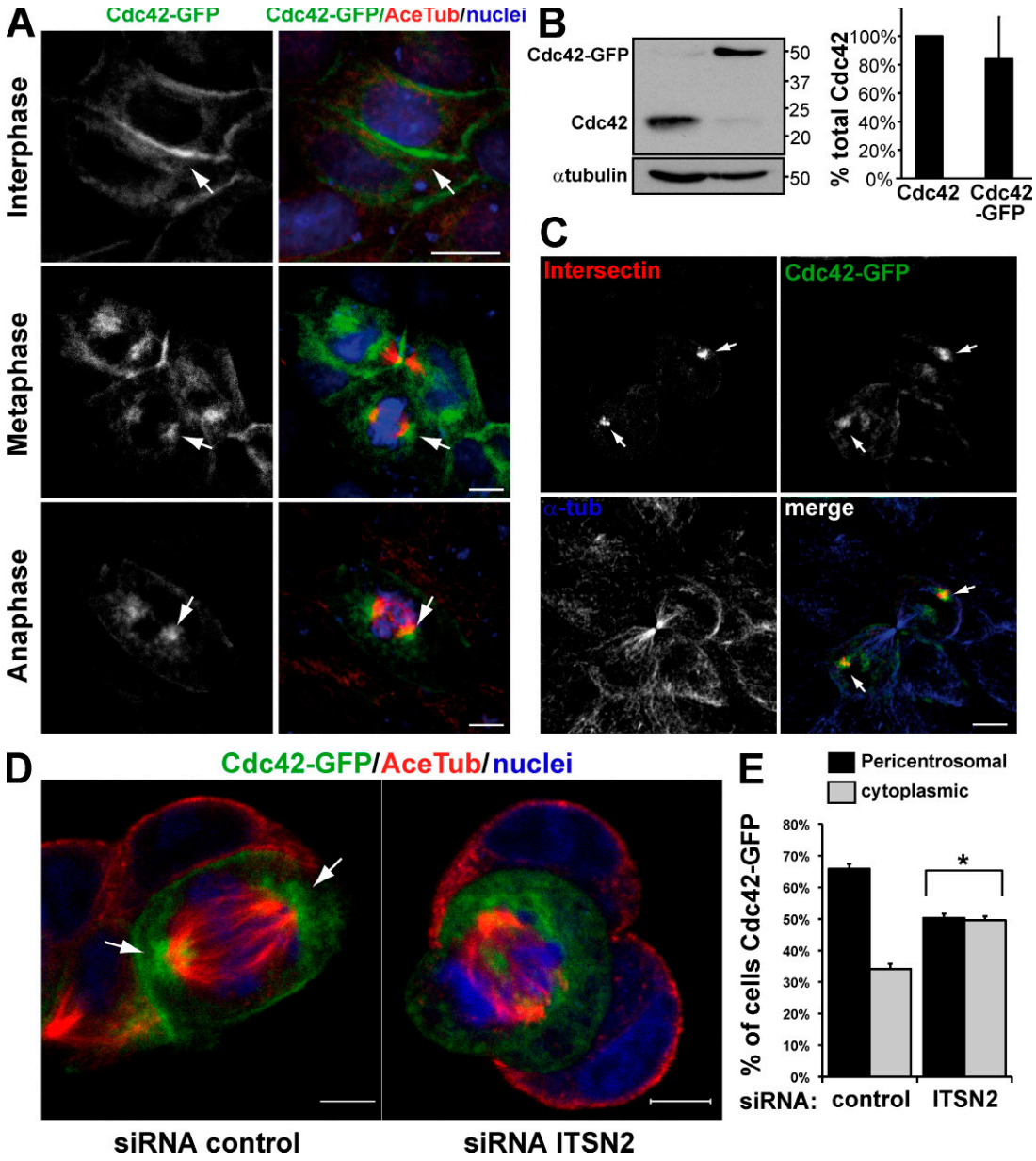

Figure 6. **Cdc42 localizes near centrosomes during mitosis.** The localization of Cdc42 in mitosis depends on ITSN2. (A) Confocal images of Cdc42 localization in MDCK cells in different phases of the cell cycle. MDCK Cdc42-GFP cells were plated in a monolayer and stained for acetylated tubulin (Ace Tub) and chromatin (blue). Cells in interphase (top), metaphase (middle), and anaphase (bottom) are shown. (B) Cdc42 levels are regulated in Cdc42-GFP cells. Total cell lysates of wild-type MDCK cells and Cdc42-GFP cells were immunoblotted for Cdc42, and total Cdc42 levels were quantified using α-tubulin as a control. Molecular mass is indicated in kilodaltons. Values shown are mean ± SD from three different experiments (Western blots). (C) Confocal images of ITSN2 colocalizing with Cdc42 in dividing cells. Cdc42-GFP cells were transfected with ITSN2-Cherry (red) and stained for α-tubulin (α-tub). Arrows indicate the localization of ITSN2 and Cdc42. (D) Confocal images showing that the localization of Cdc42 in mitosis depends on ITSN2. MDCK cells stably expressing Cdc42-GFP were silenced with siRNA oligonucleotides to ITSN2 (right) or control (left) and plated to form cysts for 24 h. Cells with Cdc42-GFP were stained for acetylated tubulin and chromatin (blue). (A and D) Arrows indicate Cdc42 localization. (E) Quantification of Cdc42-GFP associated with the mitotic spindles in control cell or cells silenced for ITSN2. Cells with Cdc42-GFP concentrated at the spindle poles or dispersed throughout the cytoplasm were quantified. Values shown are mean ± SD from three different experiments (n = 100 cysts/experiment; *, $P < 0.001$ for cytoplasmic/pericentrosomal Cdc42-GFP localization in ITSN2 KD vs. control cells). Bars, 5 μm.

Cdc42-GFP–expressing cells formed normal cysts as we showed previously (Martín-Belmonte et al., 2007). As expected, Cdc42-GFP localized mainly to the plasma membrane in interphase cells (Fig. 6 A, top); however, we detected an important fraction of Cdc42-GFP in close proximity to the mitotic spindles during different phases of cell division in MDCK cells (Fig. 6 A, middle and bottom). Interestingly, we observed that Cdc42 colocalized with ITSN2 at the mitotic spindles in dividing MDCK cells (Fig. 6 C, arrows). Therefore, during cell division, Cdc42 is localized to the region of the spindle pole and is activated by ITSN2 to control the orientation of the spindle. To investigate whether the presence of ITSN2 is necessary not only for the activation but also for the localization of Cdc42, we analyzed the effect of silencing ITSN2 on the localization of Cdc42 in MDCK cells in mitosis. In control cells, the localization of Cdc42 was concentrated at the spindle poles in cells in mitosis, but in

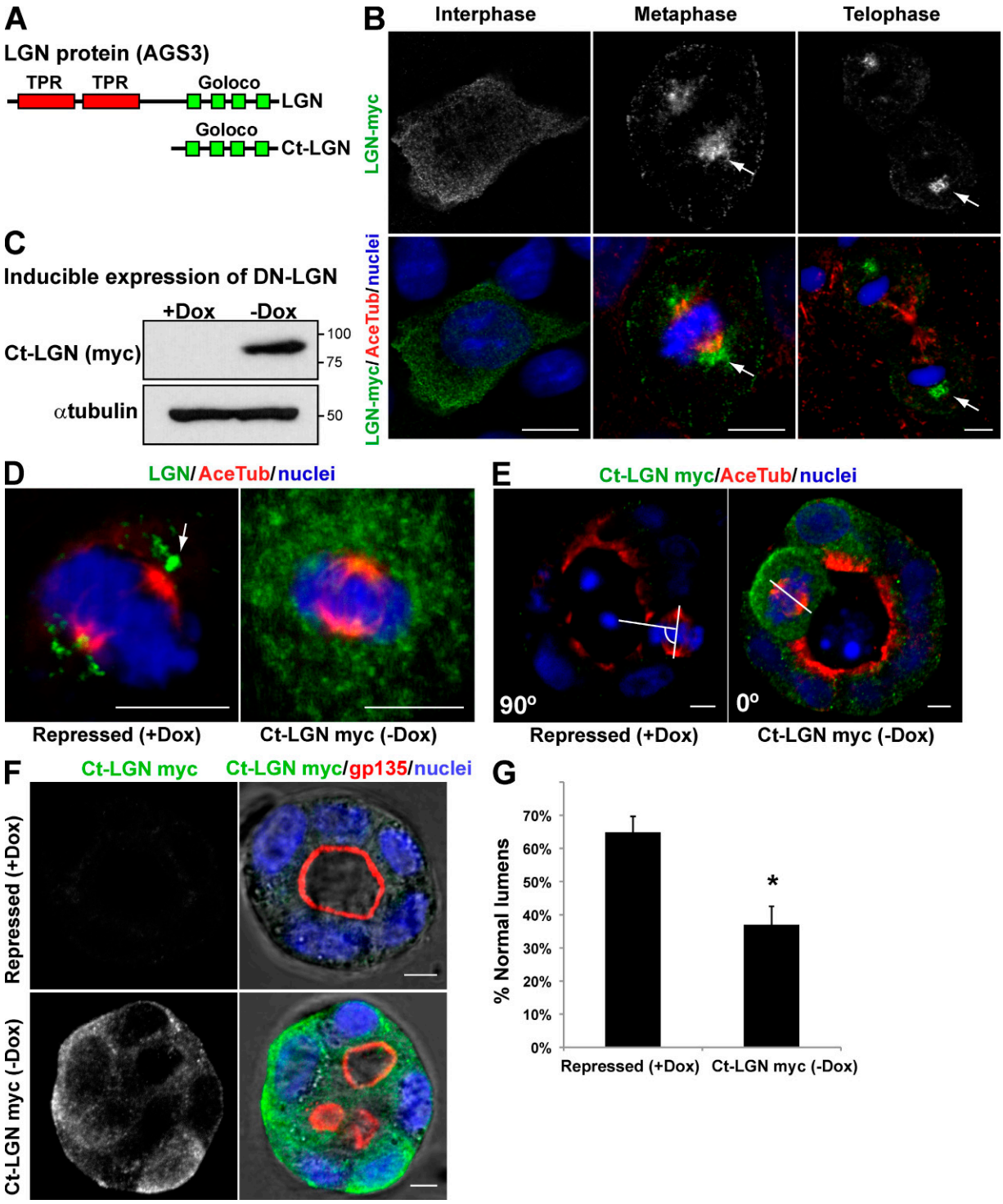

Figure 7. **Expression of a dominant-negative form of LGN in MDCK cells disrupts mitotic spindle organization in cysts and interferes with normal lumen formation.** (A) Schematic diagram of LGN protein domains and the C-terminal region (Ct-LGN) containing the four GoLoco domains that were used as the dominant-negative form of LGN. (B) Confocal images of LGN-myc localization in MDCK cells in different phases of the cell cycle. MDCK cells expressing LGN-myc (top) were plated in a monolayer and stained for acetylated tubulin (Ace Tub) and chromatin (blue; merge images in bottom panels). In cells in interphase (left), LGN localized to the cytoplasm. In cells in metaphase (middle) and telophase (right), LGN localized to the spindle poles. Arrows indicate the localization of LGN-myc. (C) Inducible expression of the dominant-negative (DN) form of LGN (Ct-LGN–myc). MDCK cells expressing Ct-LGN–myc under the control of the tet-off repressor were plated to form cysts for 72 h in the presence of Dox (Ct-LGN–myc expression repressed) or not (induced). Total lysates were Western blotted for myc (top) or α-tubulin (bottom). Molecular mass is indicated in kilodaltons. (D) Confocal microscopy images of the effect of Ct-LGN on endogenous LGN localization. Cells expressing Ct-LGN–myc were plated to form monolayers for 72 h in the presence (Ct-LGN–myc repressed) or the absence (Ct-LGN–myc induced) of 20 µmol Dox. Cells were stained to detect acetylated tubulin, LGN, and chromatin (blue). The arrow indicates the localization of LGN. (E) Confocal microscopy images of the effect of Ct-LGN on mitotic spindle orientation in cysts. Cells expressing Ct-LGN–myc were plated to form cysts for 72 h in the presence (Ct-LGN–myc repressed) or the absence (Ct-LGN–myc induced) of 20 µmol Dox. Cells were stained to detect acetylated tubulin, myc (green), and chromatin (blue). The angles between the apicobasal axis and the spindle axis (white lines) are indicated in the lower

cells silenced for ITSN2, Cdc42 was dispersed throughout the cytoplasm (Fig. 6, D [arrows] and E). These data suggest that ITSN2 is required for the localization and activation of Cdc42 at the spindle poles of mitotic cells, which in turn regulates the proper orientation of the mitotic spindle.

Disruption of LGN, a regulator of the mitotic spindle orientation, interferes with lumen formation

The data presented in this paper and previous results suggest a correlation between the orientation of the mitotic axis, regulated by Cdc42, and the formation of a single central lumen (Jaffe et al., 2008). However, to further demonstrate this relationship more convincingly, we investigated the effect of the alteration of another component of the machinery specific for mitotic spindle orientation on lumen formation. LGN, which is part of the machinery that controls the spindle orientation, contains two tetratricopeptide repeat motifs in its N-terminal region and four Gαi/o-Loco (GoLoco) motifs near the C terminus (Fig. 7 A). Tetratricopeptide repeat motifs are involved in protein–protein interactions, whereas GoLoco motifs have been implicated as inhibitors of GDP dissociation from heterotrimeric G protein α-subunits. The expression of the GoLoco motifs can act as a dominant-negative form of LGN (Ct-LGN; Fig. 7 A; Morin et al., 2007). LGN, which is expressed in MDCK cells, localizes at the cytoplasm in interphase but translocates to the cell cortex and spindle poles in mitosis (Du et al., 2001). We confirmed this localization for LGN-myc in MDCK cells (Fig. 7 B; arrows indicate LGN localization at the spindle poles). LGN regulates mitotic spindle movements and orientation, so interfering with its function randomizes the plane of division and disrupts the orientation of the mitotic spindle in epithelial and neuroepithelial cells (Du and Macara, 2004; Morin et al., 2007). To disrupt LGN function, we expressed Ct-LGN in MDCK cells under the control of an inducible promoter (tet-off; Fig. 7 C). We confirmed that Ct-LGN expression was sufficient to disperse the normal localization of LGN from the mitotic spindles (Fig. 7 D) and the normal orientation of the mitotic spindle in 3D MDCK cysts (abnormal spindles in control cells [+doxycycline (Dox)], 25.5%; abnormal spindles in Ct-LGN–induced cells [−Dox], 54.2%; Fig. 7 E), as was described previously in chick neuroepithelial cells (Morin et al., 2007). Interestingly, we also found that the expression of Ct-LGN disrupted the formation of normal lumens in MDCK cells forming cysts (Fig. 7, F and G). In sum, when we alter the orientation of the axis with the expression of a dominant-negative form of LGN, a protein essential for the orientation of the mitotic spindles in different models of cell division, the formation of the lumen results also altered. Therefore, with these experiments, we have demonstrated a direct relationship between the orientation of the mitotic axis and the formation of the lumen.

Discussion

Collectively, the results presented in this study suggest that ITSN2 is involved in the activation of Cdc42 to regulate spindle orientation during mitosis. To perform this function, ITSN2 localizes to the centrosomes, both in interphase cells and in cells in mitosis. The EH domains of ITSN2 mediate the localization of ITSN2 at the centrosomes. Thus, ITSN2 operates as a spatial regulator for Cdc42 activity, which is also associated to the spindle poles during cell division. Then, Cdc42 is required somehow for the normal function of the spindle machinery, which is involved in regulating the orientation of the mitotic spindle at the centrosomes and for the normal formation of the lumen in epithelial morphogenesis.

The mechanisms and external factors that regulate spindle orientation in epithelial cells are poorly understood. The majority of these studies have been performed using asymmetric division models (for review see Siller and Doe, 2009). However, it has been postulated that the main players of this process in mammalian epithelial cells may be the same, including the dynein–dynactin complex, Gα proteins, LGN, NuMA (nuclear mitotic apparatus protein), the Par complex, and the Rho GTPase Cdc42 (for review see Siller and Doe, 2009). The molecular mechanism associated with the function of Rho GTPases is generally related to its subcellular localization (Iden and Collard, 2008). We have shown that Cdc42 localizes to the mitotic spindle in the centrosomal region, where it can activate downstream effectors that control the mitotic spindle machinery. An essential question is how Cdc42 associates with the spindle poles. We found that ITSN2 is localized in centrosomes, through the EH domains of ITSN2. Therefore, ITSN2 could recruit and activate Cdc42 at the spindle poles. In fact, silencing of ITSN2 significantly reduces the amount of active Cdc42 and that of the Cdc42 associated with the spindle poles. In addition, ITSN2 seems to mediate protein–protein interactions with other centrosomal proteins through the SH3 domains, and thus, it might scaffold signaling platforms for Cdc42 at this location. Therefore, a potential mechanism for Cdc42 function in the orientation of the mitotic spindles might be mediated by ITSN2, which would be responsible not only for activating Cdc42 in the centrosomal region but also for scaffolding proteins involved in downstream signaling.

In addition to the data presented in this study for the role of Cdc42 by controlling mitotic spindle orientation in the MDCK cells, Cdc42 activity was also recently described to regulate epithelial morphogenesis and spindle orientation in Caco-2 cells, a mammalian intestinal model of epithelial morphogenesis (Jaffe et al., 2008). However, the link between Cdc42, spindle orientation, and the formation of the lumen described previously was strictly correlative (Jaffe et al., 2008). To clarify this issue, we have shown that disruption of LGN, a known essential component of the spindle orientation machinery, also caused a defect

left corners. (F) Confocal microscopy images of the effect of Ct-LGN in MDCK cysts on lumen formation. Cells expressing Ct-LGN–myc were plated to form cysts for 72 h in the presence (Ct-LGN–myc repressed) or the absence (Ct-LGN–myc induced) of 20 µmol Dox. Cells were stained to detect gp135, myc (green), and nuclei. (G) Quantification of cysts with normal lumens in cells expressing or not Ct-LGN–myc. Values are mean ± SD from three different experiments (n = 100 cysts/experiment; *, $P < 0.001$). Bars, 5 µm.

lumen formation similar to the defect caused by the silencing of ITSN2 and Cdc42, which suggests a direct relationship between these two processes.

The mechanism of spindle rotation may involve centrosome movement directed by interactions between the astral microtubules and the cell cortex. Therefore, the connection of astral microtubules to centrosomes and the cell cortex must be fully coordinated. A role for the actin cytoskeleton and motors such as the dynein–dynactin complex has been proposed in this process (Schuyler and Pellman, 2001; Kunda and Baum, 2009). The actin cytoskeleton is one of the main downstream effects of Rho GTPase function. To stabilize the interaction between the cell cortex, centrosomes, and the astral microtubules, Cdc42 regulates actin remodeling via different effectors such as Pak (p21-activated kinase), N-WASP, and formins in mammalian cells (Narumiya and Yasuda, 2006). Moreover, in yeast, a Cdc42 GEF complex (Bem1–cdc24p, functionally similar to ITSN) interacts with PAK and regulates the polarization of the cell division machinery (Heil-Chapdelaine et al., 1999). A previous study has elucidated a route in which Cdc42 may regulate the activation of Pak2 at the centrosomes, which in turn regulates the spindle assembly machinery, including Aurora A, dynein–dynactin, and NuMA (Mitsushima et al., 2009). In other series of experiments, Cdc42 and its effector mammalian Dia3 have been shown to regulate the biorientation of the chromosomes, which involved attachment of the plus ends of microtubules to kinetochores, to ensure alignment of chromosomes during metaphase and their correct segregation during anaphase (Yasuda et al., 2004). Therefore, although the function of Cdc42 in spindle positioning is clear, the effectors involved and the molecular mechanism acting downstream of Cdc42 remain to be identified.

Different epithelial tissues undergo events of massive membrane trafficking in the initial steps of morphogenesis (Bryant and Mostov, 2008). Previous data have demonstrated a role for Cdc42 in vesicle trafficking in polarized epithelial cells (Müsch et al., 2001). We have observed a function for Cdc42 in the exocytosis of gp135-containing vesicles and the remodeling of tight junctions in calcium switch experiments. In addition, we have found a greater effect of silencing Cdc42 on lumen formation and mitotic spindle orientation than silencing ITSN2. Our present data suggest the existence of another GEF as regulator for Cdc42 during this process. Interestingly, we have detected ITSN2 at intracellular locations in MDCK cells, which might be endosomal membranes. Multiple studies have demonstrated an important function for ITSN2 during endocytosis (Pucharcos et al., 2000; McGavin et al., 2001). Recently, it has been shown that endocytosis can act to promote cell polarity in different models (Georgiou et al., 2008, Harris and Tepass, 2008; Leibfried et al., 2008). Even more, some proteins associated with endocytosis have been described to be required for spindle positioning in mitosis (Royle et al., 2005; Liu and Zheng, 2009). The possibility that ITSN2 regulates cell polarity through endocytosis remains to be investigated.

In summary, we have identified ITSN2 as an activator of Cdc42 at the centrosomes to regulate spindle orientation during mitosis. It has been recently described that the apical membrane and the lumen originate from the place where the midbody is formed during cytokinesis (Schlüter et al., 2009). Therefore, the regulation of the orientation of the mitotic spindle, which determines the location of the midbody, would be essential to ensure the formation of a single lumen.

Materials and methods

Reagents

Antibodies against ITSN2 (Novus Biologicals), N-WASP (Santa Cruz Biotechnology, Inc.), Cdc42 (BD), pericentrin (Covance), mLGN/GPSM2/AGS3 (Abnova), α-tubulin (Sigma-Aldrich), γ-tubulin (Sigma-Aldrich), $p150^{Glued}$ (BD), GFP (Sigma-Aldrich), β-catenin (Sigma-Aldrich), and acetylated tubulin (Sigma-Aldrich) were used as primary antibodies. Gp135 antibody was a gift from the Ojakian laboratory (State University of New York Downstate Medical Center, Brooklyn, NY). Peroxidase-conjugated donkey anti–mouse IgG and anti–rabbit IgG were used as secondary antibodies for Western blots (Jackson ImmunoResearch Laboratories, Inc.). Alexa Fluor–conjugated secondary antibodies (Alexa Fluor 488, 555, or 647; Invitrogen) and TOPRO-3 (for nuclear/DNA staining) were used in microscopy protocols. Nocodazole (Sigma-Aldrich) and cytochalasin D (Sigma-Aldrich) depolymerized tubulin and actin cytoskeleton, respectively.

Vectors

N-WASP–GFP was cloned in a pEGFP-C1 vector (Takara Bio Inc.). GFP-tagged ITSN2 constructs (EH/EH, coiled-coil, SH3, and C terminus) were cloned in a pEGFP-C2 vector (Takara Bio Inc.). Human ITSN2-Cherry was a gift from S. de la Luna (Centre de Regulació Genòmica, Barcelona, Spain). Human ITSN2-L–GFP, GST-EH/EH, GST–coiled-coil, GST-5xSH3, and GST–C terminus were gifts from K. Kaibuchi (Nagoya University, Chikusa-ku, Nagoya, Japan). vhITSN2 vector was a contribution from I. Macara (University of Virginia School of Medicine, Charlottesville, VA). Myc-tagged Ct-LGN inducible and LGN-myc vector were a gift from X. Morin (École Normale Supérieure, Paris, France).

Cells

MDCK cells were grown as described previously (Martín-Belmonte et al., 2007). MDCK cells stably expressing β-tubulin–GFP, Cdc42-GFP, vhITSN2-L, inducible Cdc42V12-myc or inducible Ct-LGN–myc were made by cotransfection with blasticidin-resistant gene and selection for 10 d with 20 ng/ml Dox and 0.5 mg/ml blasticidin. To prepare cysts in Matrigel, cells were trypsinized to a single cell suspension of 2×10^4 cells/ml in 2% Matrigel and plated in coverglass chambers (Thermo Fisher Scientific) covered with Matrigel. Cysts were grown for 3–5 d.

Microscopy

Immunofluorescence of cysts was previously described (Martín-Belmonte et al., 2007). Cysts were analyzed on a confocal microscope (510 or 710 LSM; Carl Zeiss, Inc.) using a 63× NA 1.4 oil Plan-Apochromat objective and a 63× NA 1.2 water C-Apochromat Corr (for live cell and cyst imaging). The imaging acquisition system used was ZEN software suite (Carl Zeiss, Inc.). For image processing, we used ImageJ (National Institutes of Health) and ZEN software suite. For videomicroscopy and 3D reconstitutions, we processed maximum projections of all stacks and then reduced background using ImageJ software. Fixed cyst imaging was performed in PBS medium or mounted using ProLong Gold antifade reagent. Fixed cells in monolayers were analyzed in Fluoromount medium. Cysts with actin/gp135 staining at the interior surface and β-catenin facing the ECM were identified as normal lumens (interior apical pole). Cysts that had actin/gp135 absent, in small multiple lumens, or at the periphery were considered as abnormal lumens. Per condition, >100 cysts/experiment were analyzed, SD was calculated, and statistical significance was determined by paired Student's *t* test. For spindle orientation analysis, cysts were stained with acetylated tubulin, and the angle formed by the spindle and the apicobasal axis was measured. Divisions with angles <45° were considered abnormal. Per condition, >30 cysts/experiment were analyzed. For videomicroscopy, cells stably expressing β-tubulin–GFP were analyzed using an LSM 510 with incubation chamber at 5% CO_2 and 37°C. Stacks of five images were taken every 2 min, and videos were rendered at 2 frames/s from centrosome duplication until cells achieved telophase.

RNAi

25 nucleotide stealth siRNA duplexes targeting mRNA sequences of canine Cdc42 and ITSN2 were purchased from Invitrogen. Sequences were submitted to BLAST search to ensure targeting specificity. The specificity

of Cdc42 and ITSN2 was further checked by Western blot analysis. MDCK cells were trypsinized and then nucleofected (Lonza) with either Cdc42 or ITSN2 siRNA duplexes or scrambled siRNA. After 24-h incubation, cells were resuspended and plated in 12-well plates and in coverglass chambers to grow cysts. Total cell lysates were analyzed by Western blotting as described previously (Martín-Belmonte et al., 2007) to confirm siRNA efficiency.

Calcium switch and microtubule repolymerization assays

Calcium switch was performed by incubating cells overnight in a calcium-free MEM medium (supplemented with dialyzed FCS) and then restoring normal calcium conditions with complete MEM for 120 min. Microtubule depolymerization was performed by incubating cells in 20 µg/ml nocodazole-supplemented MEM for 240 min. Then, nocodazole was washed out by incubating cells in normal MEM for 15–45 min.

Centrosome purification

Centrosomes were purified using fast isolation of centrosomes (Blomberg-Wirschell and Doxsey, 1998). 5×10^8 cells were treated during 180 min with 20 µg/ml nocodazole and 1 µg/ml cytochalasin D. Cells were washed in cold PBS, 8% sucrose, 0.1× PBS, and then 8% sucrose and finally lysed using 0.5% Triton X-100 and 0.1% 2-mercaptoethanol in Tris-HCl buffer, pH 8.0, for 10 min at 4°C. Cell debris and nuclei were removed by fast centrifugation at 1,500 *g* for 5 min at 4°C and 33-µm filters. The lysate was loaded on top of a 1.5-ml 20% Ficoll 400 cushion and centrifuged at 25,000 *g* for 20 min at 4°C. Five 1-ml fractions were collected, and then fractions were diluted 1:4 in Pipes-EDTA buffer and centrifuged at 25,000 *g* for 20 min at 4°C. The sediment was resuspended in Laemmli buffer and loaded. Supernatants and top fractions were loaded as control.

GTPase activation

Cysts were lysed in 500 µl of 4°C 2× gold lysis buffer (2% Triton X-100, 40 mM Tris HCl, pH 7.5, 150 mM NaCl, 20 mM $MgCl_2$, 30% glycerol, 1 mM DTT, and EDTA-free protease inhibitors; Roche) and centrifuged at 15,000 rpm for 5 min. A 50-µl sample from the supernatant was set aside for determination of Cdc42 and tubulin levels in the total lysate, and GTP loading on Cdc42 was determined with GST-Pak3-CRIB pull-down.

ITSN2 pull-down assays

Cysts grown in 100,000 cells/ml on top of Matrigel-coated dishes were lysed in 0.1% SDS, 1% Triton X-100, 0.5 mM DTT, and 1× TBS buffer with protease inhibitor cocktail and NaOV. Cell debris was removed by fast cold centrifugation at 14,000 *g* for 2 min, and cleared lysates were incubated in rotation with protein-GST–loaded beads for 30 min. Beads were centrifuged and washed four times, dried using aspiration, and resuspended in Laemmli buffer.

Online supplemental material

Fig. S1 shows the effect of ITSN2 silencing using stable short hairpin RNA expression. Fig. S2 shows that ITSN2 localization to centrosomes is independent of microtubules. Fig. S3 shows that MTOC orientation is not affected by ITSN2 or Cdc42 silencing. Videos 1, 2, and 3 show spindle dynamics in control MDCK, ITSN2-silenced, and Cdc42-silenced cells, respectively. Online supplemental material is available at http://www.jcb.org/cgi/content/full/jcb.201002047/DC1.

We thank C.M. Ruiz-Jarabo and I. Correas for comments on the manuscript and members of the F. Martín-Belmonte, J. Millán, and M.A. Alonso laboratories for discussion. We also thank I. Macara for the plasmid of vhITSN2, X. Morin for the plasmids of LGN-myc and CH-LGN–myc, S. de la Luna for the plasmid of hITSN2, and K. Kaibuchi for the plasmids of GST-tagged domains of ITSN2.

This work was supported by grants from the Human Frontier Science Program (HFSP-CDA 00011/2009) and Marie Curie (IRG-209382) to F. Martín-Belmonte, National Institutes of Health grants (R01 DK067153 and R01 DK074398) to K. Mostov, and grants from the Ministerio de Ciencia e Innovación to F. Martín-Belmonte (BFU2008-01916) and M.A. Alonso (BFU2006-01925) and to F. Martín-Belmonte and M.A. Alonso (CONSOLIDER CSD2009-00016). An institutional grant from the Fundación Ramón Areces to the Centro de Biología Molecular Severo Ochoa is also acknowledged.

Submitted: 9 February 2010
Accepted: 20 April 2010

Note added in proof. In this issue, Qin et al. (2010. *J. Cell Biol.* doi:10.1083/jcb.201002097) have characterized the role of Tuba, another GEF specific for Cdc42, to be involved in spindle orientation and epithelial cyst formation, suggesting that Cdc42 must be regulated at different levels to control epithelial morphogenesis.

Also, during the editing process, Zheng et al. (2010. *J. Cell Biol.* doi:10.1083/jcb.200910021) characterized the role of LGN in spindle orientation and epithelial cyst formation, which corroborates the results presented in this paper.

References

Blomberg-Wirschell, M., and S.J. Doxsey. 1998. Rapid isolation of centrosomes. *Methods Enzymol.* 298:228–238. doi:10.1016/S0076-6879(98)98022-3

Bryant, D.M., and K.E. Mostov. 2008. From cells to organs: building polarized tissue. *Nat. Rev. Mol. Cell Biol.* 9:887–901. doi:10.1038/nrm2523

Du, Q., and I.G. Macara. 2004. Mammalian Pins is a conformational switch that links NuMA to heterotrimeric G proteins. *Cell*. 119:503–516. doi:10.1016/j.cell.2004.10.028

Du, Q., P.T. Stukenberg, and I.G. Macara. 2001. A mammalian Partner of inscuteable binds NuMA and regulates mitotic spindle organization. *Nat. Cell Biol.* 3:1069–1075. doi:10.1038/ncb1201-1069

Etienne-Manneville, S. 2004. Cdc42—the centre of polarity. *J. Cell Sci.* 117:1291–1300. doi:10.1242/jcs.01115

Georgiou, M., E. Marinari, J. Burden, and B. Baum. 2008. Cdc42, Par6, and aPKC regulate Arp2/3-mediated endocytosis to control local adherens junction stability. *Curr. Biol.* 18:1631–1638. doi:10.1016/j.cub.2008.09.029

Gomes, E.R., S. Jani, and G.G. Gundersen. 2005. Nuclear movement regulated by Cdc42, MRCK, myosin, and actin flow establishes MTOC polarization in migrating cells. *Cell*. 121:451–463. doi:10.1016/j.cell.2005.02.022

Harris, K.P., and U. Tepass. 2008. Cdc42 and Par proteins stabilize dynamic adherens junctions in the *Drosophila* neuroectoderm through regulation of apical endocytosis. *J. Cell Biol.* 183:1129–1143. doi:10.1083/jcb.200807020

Heil-Chapdelaine, R.A., N.R. Adames, and J.A. Cooper. 1999. Formin' the connection between microtubules and the cell cortex. *J. Cell Biol.* 144:809–811. doi:10.1083/jcb.144.5.809

Hung, L.Y., C.J. Tang, and T.K. Tang. 2000. Protein 4.1 R-135 interacts with a novel centrosomal protein (CPAP) which is associated with the gamma-tubulin complex. *Mol. Cell. Biol.* 20:7813–7825. doi:10.1128/MCB.20.20.7813-7825.2000

Hurd, T.W., L. Gao, M.H. Roh, I.G. Macara, and B. Margolis. 2003. Direct interaction of two polarity complexes implicated in epithelial tight junction assembly. *Nat. Cell Biol.* 5:137–142. doi:10.1038/ncb923

Hussain, N.K., S. Jenna, M. Glogauer, C.C. Quinn, S. Wasiak, M. Guipponi, S.E. Antonarakis, B.K. Kay, T.P. Stossel, N. Lamarche-Vane, and P.S. McPherson. 2001. Endocytic protein intersectin-l regulates actin assembly via Cdc42 and N-WASP. *Nat. Cell Biol.* 3:927–932. doi:10.1038/ncb1001-927

Iden, S., and J.G. Collard. 2008. Crosstalk between small GTPases and polarity proteins in cell polarization. *Nat. Rev. Mol. Cell Biol.* 9:846–859. doi:10.1038/nrm2521

Irie, F., and Y. Yamaguchi. 2002. EphB receptors regulate dendritic spine development via intersectin, Cdc42 and N-WASP. *Nat. Neurosci.* 5:1117–1118. doi:10.1038/nn964

Itoh, R.E., K. Kurokawa, Y. Ohba, H. Yoshizaki, N. Mochizuki, and M. Matsuda. 2002. Activation of rac and cdc42 video imaged by fluorescent resonance energy transfer-based single-molecule probes in the membrane of living cells. *Mol. Cell. Biol.* 22:6582–6591. doi:10.1128/MCB.22.18.6582-6591.2002

Jaffe, A.B., and A. Hall. 2005. Rho GTPases: biochemistry and biology. *Annu. Rev. Cell Dev. Biol.* 21:247–269. doi:10.1146/annurev.cellbio.21.020604.150721

Jaffe, A.B., N. Kaji, J. Durgan, and A. Hall. 2008. Cdc42 controls spindle orientation to position the apical surface during epithelial morphogenesis. *J. Cell Biol.* 183:625–633. doi:10.1083/jcb.200807121

Joberty, G., C. Petersen, L. Gao, and I.G. Macara. 2000. The cell-polarity protein Par6 links Par3 and atypical protein kinase C to Cdc42. *Nat. Cell Biol.* 2:531–539. doi:10.1038/35019573

Kroschewski, R., A. Hall, and I. Mellman. 1999. Cdc42 controls secretory and endocytic transport to the basolateral plasma membrane of MDCK cells. *Nat. Cell Biol.* 1:8–13. doi:10.1038/8977

Kunda, P., and B. Baum. 2009. The actin cytoskeleton in spindle assembly and positioning. *Trends Cell Biol.* 19:174–179. doi:10.1016/j.tcb.2009.01.006

Lee, M., and V. Vasioukhin. 2008. Cell polarity and cancer—cell and tissue polarity as a non-canonical tumor suppressor. *J. Cell Sci.* 121:1141–1150. doi:10.1242/jcs.016634

Leibfried, A., R. Fricke, M.J. Morgan, S. Bogdan, and Y. Bellaiche. 2008. *Drosophila* Cip4 and WASp define a branch of the Cdc42-Par6-aPKC pathway regulating E-cadherin endocytosis. *Curr. Biol.* 18:1639–1648. doi:10.1016/j.cub.2008.09.063

Liu, Z., and Y. Zheng. 2009. A requirement for epsin in mitotic membrane and spindle organization. *J. Cell Biol.* 186:473–480. doi:10.1083/jcb.200902071

Lo, C.M., C.R. Keese, and I. Giaever. 1995. Impedance analysis of MDCK cells measured by electric cell-substrate impedance sensing. *Biophys. J.* 69:2800–2807. doi:10.1016/S0006-3495(95)80153-0

Malacombe, M., M. Ceridono, V. Calco, S. Chasserot-Golaz, P.S. McPherson, M.F. Bader, and S. Gasman. 2006. Intersectin-1L nucleotide exchange factor regulates secretory granule exocytosis by activating Cdc42. *EMBO J.* 25:3494–3503. doi:10.1038/sj.emboj.7601247

Martín-Belmonte, F., A. Gassama, A. Datta, W. Yu, U. Rescher, V. Gerke, and K. Mostov. 2007. PTEN-mediated apical segregation of phosphoinositides controls epithelial morphogenesis through Cdc42. *Cell*. 128:383–397. doi:10.1016/j.cell.2006.11.051

Martín-Belmonte, F., W. Yu, A.E. Rodríguez-Fraticelli, A.J. Ewald, A. Ewald, Z. Werb, M.A. Alonso, and K. Mostov. 2008. Cell-polarity dynamics controls the mechanism of lumen formation in epithelial morphogenesis. *Curr. Biol.* 18:507–513. doi:10.1016/j.cub.2008.02.076

McGavin, M.K., K. Badour, L.A. Hardy, T.J. Kubiseski, J. Zhang, and K.A. Siminovitch. 2001. The intersectin 2 adaptor links Wiskott Aldrich Syndrome protein (WASp)-mediated actin polymerization to T cell antigen receptor endocytosis. *J. Exp. Med.* 194:1777–1787. doi:10.1084/jem.194.12.1777

Mitsushima, M., F. Toyoshima, and E. Nishida. 2009. Dual role of Cdc42 in spindle orientation control of adherent cells. *Mol. Cell. Biol.* 29:2816–2827. doi:10.1128/MCB.01713-08

Morin, X., F. Jaouen, and P. Durbec. 2007. Control of planar divisions by the G-protein regulator LGN maintains progenitors in the chick neuroepithelium. *Nat. Neurosci.* 10:1440–1448. doi:10.1038/nn1984

Müsch, A., D. Cohen, G. Kreitzer, and E. Rodriguez-Boulan. 2001. cdc42 regulates the exit of apical and basolateral proteins from the trans-Golgi network. *EMBO J.* 20:2171–2179. doi:10.1093/emboj/20.9.2171

Narumiya, S., and S. Yasuda. 2006. Rho GTPases in animal cell mitosis. *Curr. Opin. Cell Biol.* 18:199–205. doi:10.1016/j.ceb.2006.02.002

O'Brien, L.E., T.S. Jou, A.L. Pollack, Q. Zhang, S.H. Hansen, P. Yurchenco, and K.E. Mostov. 2001. Rac1 orientates epithelial apical polarity through effects on basolateral laminin assembly. *Nat. Cell Biol.* 3:831–838. doi:10.1038/ncb0901-831

Okamoto, M., S. Schoch, and T.C. Südhof. 1999. EHSH1/intersectin, a protein that contains EH and SH3 domains and binds to dynamin and SNAP-25. A protein connection between exocytosis and endocytosis? *J. Biol. Chem.* 274:18446–18454. doi:10.1074/jbc.274.26.18446

Palazzo, A.F., H.L. Joseph, Y.J. Chen, D.L. Dujardin, A.S. Alberts, K.K. Pfister, R.B. Vallee, and G.G. Gundersen. 2001. Cdc42, dynein, and dynactin regulate MTOC reorientation independent of Rho-regulated microtubule stabilization. *Curr. Biol.* 11:1536–1541. doi:10.1016/S0960-9822(01)00475-4

Pucharcos, C., X. Estivill, and S. de la Luna. 2000. Intersectin 2, a new multimodular protein involved in clathrin-mediated endocytosis. *FEBS Lett.* 478:43–51. doi:10.1016/S0014-5793(00)01793-2

Quintyne, N.J., S.R. Gill, D.M. Eckley, C.L. Crego, D.A. Compton, and T.A. Schroer. 1999. Dynactin is required for microtubule anchoring at centrosomes. *J. Cell Biol.* 147:321–334. doi:10.1083/jcb.147.2.321

Rescher, U., and V. Gerke. 2004. Annexins—unique membrane binding proteins with diverse functions. *J. Cell Sci.* 117:2631–2639. doi:10.1242/jcs.01245

Rojas, R., W.G. Ruiz, S.M. Leung, T.S. Jou, and G. Apodaca. 2001. Cdc42-dependent modulation of tight junctions and membrane protein traffic in polarized Madin-Darby canine kidney cells. *Mol. Biol. Cell*. 12:2257–2274.

Royle, S.J., N.A. Bright, and L. Lagnado. 2005. Clathrin is required for the function of the mitotic spindle. *Nature*. 434:1152–1157. doi:10.1038/nature03502

Schlüter, M.A., C.S. Pfarr, J. Pieczynski, E.L. Whiteman, T.W. Hurd, S. Fan, C.J. Liu, and B. Margolis. 2009. Trafficking of Crumbs3 during cytokinesis is crucial for lumen formation. *Mol. Biol. Cell*. 20:4652–4663. doi:10.1091/mbc.E09-02-0137

Schuyler, S.C., and D. Pellman. 2001. Search, capture and signal: games microtubules and centrosomes play. *J. Cell Sci.* 114:247–255.

Siller, K.H., and C.Q. Doe. 2009. Spindle orientation during asymmetric cell division. *Nat. Cell Biol.* 11:365–374. doi:10.1038/ncb0409-365

Vega-Salas, D.E., P.J. Salas, and E. Rodriguez-Boulan. 1987. Modulation of the expression of an apical plasma membrane protein of Madin-Darby canine kidney epithelial cells: cell-cell interactions control the appearance of a novel intracellular storage compartment. *J. Cell Biol.* 104:1249–1259. doi:10.1083/jcb.104.5.1249

Vega-Salas, D.E., P.J. Salas, and E. Rodriguez-Boulan. 1988. Exocytosis of vacuolar apical compartment (VAC): a cell-cell contact controlled mechanism for the establishment of the apical plasma membrane domain in epithelial cells. *J. Cell Biol.* 107:1717–1728. doi:10.1083/jcb.107.5.1717

Wells, C.D., J.P. Fawcett, A. Traweger, Y. Yamanaka, M. Goudreault, K. Elder, S. Kulkarni, G. Gish, C. Virag, C. Lim, et al. 2006. A Rich1/Amot complex regulates the Cdc42 GTPase and apical-polarity proteins in epithelial cells. *Cell*. 125:535–548. doi:10.1016/j.cell.2006.02.045

Wu, H., G. Rossi, and P. Brennwald. 2008. The ghost in the machine: small GTPases as spatial regulators of exocytosis. *Trends Cell Biol.* 18:397–404. doi:10.1016/j.tcb.2008.06.007

Yamabhai, M., N.G. Hoffman, N.L. Hardison, P.S. McPherson, L. Castagnoli, G. Cesareni, and B.K. Kay. 1998. Intersectin, a novel adaptor protein with two Eps15 homology and five Src homology 3 domains. *J. Biol. Chem.* 273:31401–31407. doi:10.1074/jbc.273.47.31401

Yasuda, S., F. Oceguera-Yanez, T. Kato, M. Okamoto, S. Yonemura, Y. Terada, T. Ishizaki, and S. Narumiya. 2004. Cdc42 and mDia3 regulate microtubule attachment to kinetochores. *Nature*. 428:767–771. doi:10.1038/nature02452

Yoshizaki, H., Y. Ohba, K. Kurokawa, R.E. Itoh, T. Nakamura, N. Mochizuki, K. Nagashima, and M. Matsuda. 2003. Activity of Rho-family GTPases during cell division as visualized with FRET-based probes. *J. Cell Biol.* 162:223–232. doi:10.1083/jcb.200212049

Yu, W., L.E. O'Brien, F. Wang, H. Bourne, K.E. Mostov, and M.M. Zegers. 2003. Hepatocyte growth factor switches orientation of polarity and mode of movement during morphogenesis of multicellular epithelial structures. *Mol. Biol. Cell*. 14:748–763. doi:10.1091/mbc.E02-06-0350

Yu, W., A. Datta, P. Leroy, L.E. O'Brien, G. Mak, T.S. Jou, K.S. Matlin, K.E. Mostov, and M.M. Zegers. 2005. Beta1-integrin orients epithelial polarity via Rac1 and laminin. *Mol. Biol. Cell*. 16:433–445. doi:10.1091/mbc.E04-05-0435

Yu, W., A.M. Shewan, P. Brakeman, D.J. Eastburn, A. Datta, D.M. Bryant, Q.W. Fan, W.A. Weiss, M.M. Zegers, and K.E. Mostov. 2008. Involvement of RhoA, ROCK I and myosin II in inverted orientation of epithelial polarity. *EMBO Rep.* 9:923–929. doi:10.1038/embor.2008.135